IEEE Access
Multidisciplinary | Rapid Review | Open Access Journal

Received September 3, 2020, accepted September 18, 2020, date of publication September 28, 2020,
date of current version October 8, 2020.

Digital Object Identifier 10.1109/ACCESS.2020.3027052

Fixed-Time Backstepping Control of Quadrotor Trajectory Tracking Based On Neural Network

MINGYU WANG, BING CHEN, AND CHONG LIN, (Senior Member, IEEE)
Institute of Complexity Science, Qingdao University, Qingdao 266071, China
Shandong Key Laboratory of Industrial Control Technology, Qingdao University, Qingdao 266071, China

Corresponding author: Bing Chen (chenbing1958@126.com)

This work was supported by the National Natural Science Foundation of China under Grant 61873137 and Grant 61673227.

ABSTRACT This paper aims at the trajectory tracking of a quadrotor. A novel fixed-time backstepping control design scheme is proposed for the quadrotor based on adaptive neural control approach. The suggested adaptive controller ensures that the quadrotor well tracks the desired trajectory in finite time in spite of appearance of model uncertainties. Finally, simulation results are given to verify the effectiveness of the proposed control strategy.

INDEX TERMS Fixed-time adaptive neural control, backstepping, quadcopter, trajectory tracking.

I. INTRODUCTION

Due to its exquisite structure, the quadrotor can flexibly vertically takeoff and landing. So, the quadrotor is applied to various engineering fields such as fire rescue, logistics and transportation, and electric power patrol, and so on. These tasks inevitably involve the issue of track tracking of the quadrotor. In addition, the modeling uncertainty and the strong coupling of nonlinearities pose great challenges for controlling the four-rotor aircrafts.

In [1] and [2], the authors propose an adaptive fuzzy trajectory tracking control scheme for a quadrotor. With respective to nonlinearity, strong coupling and sensitivity to interference, a double closed-loop auto-disturbance rejection control scheme is proposed to achieve the target trajectory tracking. In [3], adaptive neural sliding mode technique is applied to quadrotor. The proposed control law guarantees achievement of position tracking and attitude tracking of the quadrotors. Similar sliding mode-based trajectory tracking control schemes are proposed for quad-rotor systems in [4] and [5], respectively. The work in [6] discusses the trajectory tracking control of the quadrotor by Type-2 fuzzy model approach. In [7], the authors propose a direct adaptive backstepping control strategy. In these works, the dynamics of quadrotor is formulated by the linear approximation relationship between Euler angle and angular velocity of the body. When quadrotor flies at a large angle, the linear relationship does not meet the requirements of the quadrotor's flying. Because of ignoring inherent nonlinearities of quadrotor, the designed controllers in light of linear approximation relationship may not work well. Therefore, some researchers set up the quadrotor model by considering the nonlinear relationship between Euler angle and angular velocity. In [8], the quadrotor system is considered as two interrelated subsystems, and a proportional integral-derivative H_∞ controller is presented. In addition, other control methods, including hierarchical control strategy [9], robust output feedback [10], [11] and integral sliding mode method [12], [13], are utilized to design the trajectory tracking controller for a quadrotor.

The aforementioned control strategies just achieve the asymptotically tracking control. That means the good tracking performance is achieved during a process of time variable t tending to infinity. In practice, such an asymptotic process may not satisfy the requirement of achieving fast tracking. Therefore, some finite-time trajectory tracking control strategies are developed. The trajectory tracking problem of a quadrotor with finite-time convergence is studied in [14]. The work in [15] proposes a cascaded sliding mode control(CSMC) method to realize finite-time trajectory tracking control. The finite-time control strategy proposed in [16] further considers the effect of state delays in system models. By using cascade sliding mode control technique, a finite-time trajectory tracking controller is developed for quadrotor aircrafts in [17]. The robust finite-time attitude tracking control is discussed in [18] by using a non-singular

The associate editor coordinating the review of this manuscript and approving it for publication was Min Wang.

terminal sliding mode approach. A non-overestimation adaptive multi-variable controller is given in [19], which is helpful to reduce chattering caused by sliding mode. The work in [20] further considers the case of velocity measurement being unavailable. A finite-time tracking controller is developed based on velocity observer. Recently, an adaptive neural finite-time robust control strategy is presented for quadrotor with input saturation via backstepping in [21].

Usually, the convergence time estimation of conventional finite-time control algorithms depends on the initial conditions. But that of fixed-time control algorithms is independent of the initial conditions and can be predefined by the users. A fixed-time tracking control scheme is proposed in [22]. The suggested fixed-time sliding mode controller achieves the trajectory tracking in fixed time. However, in the existing finite-time or fixed-time control strategies for quadrotors, the usage of symbol function leads to the corresponding control laws being non-smooth. In addition, when backstepping is used to construct a finite-time tracking control law, the designed virtual control signals always contain an error feedback term with a power exponent less than 1. As a result, in the next design step the derivative of that item will cause singularity at the origin.

Based on the above discussion, this paper still focuses on fixed-time trajectory tracking control of quadrotors. In control design procedure, the system model uncertainty is considered. Neural networks are used to model the unknown nonlinear system functions. Furthermore, a systemic adaptive neural backstepping fixed-time trajectory tracking control design process is proposed. By using polynomial interpolation, a novel smooth fixed-time adaptive neural tracking control law is constructed, which ensures to achieve trajectory tracking control of a quadrotor. Since the proposed control law is smooth, the problems of controller tremble and singularity of the derivatives of virtual control signals are successfully avoided. Based on Lyapunov stability theory, it is shown that the proposed controller ensures the tracking errors converge to a small neighborhood around origin in fixed time, and all the closed-loop signals remain bounded. At last, a numerical simulation is given to test the availability of our results.

II. PROBLEM FORMULATION

A. QUADCOPTER MODEL

To describe the motion of a quadrotor in space, Ξ_E denotes the earth's fixed coordinate system, Ξ_B refers to the fixed coordinate system of the body of quadrotor and e_3 is the unit vector of the z axis of Ξ_B. The rotation matrix R is given by

$$R = \begin{bmatrix} c\theta c\psi & c\theta c\psi & -s\theta \\ s\phi s\theta c\psi - c\phi s\psi & s\phi s\theta s\psi + c\phi c\psi & s\phi c\theta \\ c\phi s\theta s\psi + s\phi s\psi & c\phi s\theta s\psi - s\phi c\psi & c\phi c\theta \end{bmatrix} \quad (1)$$

where $c\phi = cos\phi$, $c\theta = cos\theta$, $c\psi = cos\psi$, $s\phi = sin\phi$, $s\theta = sin\theta$, $s\psi = sin\psi$, ϕ, θ and ψ are roll angle, pitch angle and yaw angle, respectively. Furthermore, the Euler angle is defined as $\Theta = [\phi, \theta, \psi]^T$.

The position of the center of mass is defined as $P = [x, y, z]^T$ in the Ξ_E, and $V = [u, v, w]^T$ is the velocity vector of the center of mass relative to Ξ_E. Let U_1 denote the total lift, g be the acceleration of gravity, $f_{uc} = [f_{ucx}, f_{ucy}, f_{ucz}]^T$ be the uncertain resistance of quadrotor during flight and $\tau_{uc} = [\tau_{ucx}, \tau_{ucy}, \tau_{ucz}]^T$ refer to uncertainty during the rotation of the quadrotor, which is the rotor gyro torque. Let $\Omega = [p, q, r]^T$ stand for the angular velocity vector and $J = diag(J_x, J_y, J_z)$ be the diagonal inertia matrix. Three virtual controllers, i.e., U_x, U_y, U_z, of the position system are defined as follows.

$$\begin{bmatrix} U_x \\ U_y \\ U_z \end{bmatrix} = \begin{bmatrix} \frac{1}{m}U_1(cos\phi cos\psi sin\theta + sin\psi sin\phi) \\ \frac{1}{m}U_1(cos\phi sin\psi sin\theta - cos\psi sin\phi) \\ \frac{1}{m}(U_1(cos\phi cos\theta) - mg) \end{bmatrix} \quad (2)$$

Remark 1: With the virtual controllers defined in (2), if the desired yaw angle ψ_d is given, then the desired lift U_1, roll angle ϕ_d and pitch angle θ_d can be given by

$$\begin{aligned} U_1 &= m\sqrt{U_x^2 + U_y^2 + (U_z + g)^2} \\ \phi_d &= arcsin(\frac{m(U_x sin\psi_d - U_y cos\psi_d)}{U_1}) \\ \theta_d &= arctan(\frac{U_x cos\psi_d + U_y sin\psi_d}{U_z + g}) \end{aligned} \quad (3)$$

Thus, let $X_1 = [\phi, \theta, \psi]^T$, $Y_1 = [p, q, r]^T$ and $U = [U_2, U_3, U_4]^T$, where U_2, U_3, and U_4 are the roll moment, pitch moment and yaw moment, respectively. Then, the attitude control system is described as

$$\begin{aligned} \dot{X}_1 &= F_1(X_1, Y_1) + \Lambda_1 Y_1 \\ \dot{Y}_1 &= S_1 F_2(X_2) + B\tau + \tilde{S}_1 U \end{aligned} \quad (4)$$

where $F_1(X_1, Y_1) = [f_{11}, f_{12}, f_{13}]^T$, $\Lambda_1 = diag(1, cos\phi, cos\phi/cos\theta)$, $f_{11} = tan\theta(qsin\phi + rcos\phi)$, $f_{12} = -rsin\phi$, $f_{13} = (sin\phi/cos\theta)q$, $f_{21} = qr$, $f_{22} = pr$, $f_{23} = pq$, $F_2(X_2) = [f_{21}, f_{22}, f_{23}]^T$, $\tau = [\tau_{ucx}, \tau_{ucy}, \tau_{ucz}]^T$, $\tilde{S}_1 = diag(1/J_x, 1/J_y, 1/J_z)$, $U = (U_2, U_3, U_4)^T$, $S_1 = diag((J_y - J_z)/J_x, (J_z - J_x)/J_y, (J_x - J_y)/J_z)$ and $B = diag(1/J_x, 1/J_y, 1/J_z)$.

And let $X_2 = [x, y, z]^T$, $Y_2 = [u, v, w]^T$, $F_{uc} = [f_{ucx}, f_{ucy}, f_{ucz} - g]^T$, $\tilde{U} = [U_x, U_y, U_z]^T$ and $\Lambda_2 = diag(-\frac{1}{m}, -\frac{1}{m}, -\frac{1}{m})$. Then, the position control system can be described by

$$\begin{aligned} \dot{X}_2 &= Y_2 \\ \dot{Y}_2 &= \Lambda_2 F_{uc} + \tilde{U} \end{aligned} \quad (5)$$

Figure 1 is the control flow chart of this article, where x stands for system status.

In order to facilitate subsequent research, the following necessary assumptions and lemmas are introduced.

Assumption 1. Quadcopter is a rigid body.

Assumption 2*:* Mass and moment of inertia are constant.

Assumption 3*:* Quadcopter geometric center is consistent with the center of gravity.

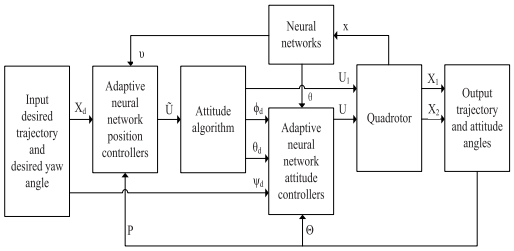

FIGURE 1. Control flow chart.

Lemma 1 *[23]:* Let $0 < s = \frac{s_1}{s_2} \leq 1$ with s_1, s_2 being two odd integers, $\tilde{a} = a - b$. Then, the following inequality holds

$$\tilde{a}(a-\tilde{a})^s \leq \gamma_1 a^{1+s} - \gamma_2 \tilde{a}^{1+s} \tag{6}$$

where $\gamma_1 = \frac{1}{1+s}(1 - 2^{2s-1} + \frac{1}{1+s}s + \frac{1}{1+s}2^s\ (1 - s^2))$ and $\gamma_2 = \frac{2^{s-1}}{1+s}(1 - 2^{s(s-1)})$.

Lemma 2 *[24]:* For a continuous nonlinear function $f(Z)$ over a compact set $\Omega_z \subset R^q$, there exists a RBF NN $S(Z)W^*$ such that for a desired level of accuracy $\bar{\delta} > 0$

$$f(Z) = S(Z)W^* + \delta(Z), \mid \delta(Z) \mid \leq \bar{\delta} \tag{7}$$

where W^* is the ideal constant weight vector and defined as

$$W^* := arg \min_{W \in \overline{R}^l} \sup_{Z \in \Omega_z} \{\mid f(Z) - S(Z)W^* \mid\} \tag{8}$$

and $\delta(Z)$ denotes the approximation error and $S(Z)$ means the basis function vector of the RBF NNs. For the definite l (the number of RBF NN nodes and $l > 1$), W^* and $S(Z)$ have the following form $W^* = [\omega_1, \omega_2, \ldots, \omega_l]^T \in R^l$, $S(Z) = [s_1(Z), s_2(Z), \ldots, s_l(Z)]$ with $s_i(Z)$ being the Gaussian function below.

$$s_i(Z) = exp\left[-\frac{(Z-\mu_i)^T(Z-\mu_i)}{\eta^2}\right] \tag{9}$$

where $\mu_i = [\mu_{i1}, \mu_{i2}, \ldots, \mu_{iq}]^T, i = 1, \ldots, l$, are the centers of the receptive field and η is the width of the Gaussian function.

Lemma 3 *[25]:* For $\forall \omega \geq x \geq 0$, and $q > 1$, the following inequality is satisfied:

$$x(\omega - x)^q \leq \frac{q}{q+1}(\omega^{q+1} - x^{q+1}) \tag{10}$$

Lemma 4 *[25]:* Consider system $\dot{x} = f(x)$ with the origin being the equilibrium point. If there exists a continuous radially unbounded and positive definite function $V(x)$, such that $\dot{V}(x) \leq -\alpha V^p(x) - \beta V^q(x) + d$ for some $\alpha > 0$, $\beta > 0$, $p > 1$, $0 < q < 1$, $0 < \eta < 1$ and d representing the constant, then, the point of the system is fixed-time stable and the settling time function T is given by

$$T \leq T_{max} := \frac{1}{\eta\alpha(p-1)} + \frac{1}{\eta\beta(1-q)} \tag{11}$$

Lemma 5 *[26]:* Let a_i be positive constants, for $1 \leq i \leq n, n \in N^+$ and $0 < k \leq 1$. Then

$$(\sum_{i=1}^{n} a_i)^k \leq \sum_{i=1}^{n} a_i^k \leq n^{1-k}(\sum_{i=1}^{n} a_i)^k. \tag{12}$$

Lemma 6 *[27]:* For $a_i \geq 0$, $k > 1$,and $n \in N^+$, one has

$$n^{1-k}(\sum_{i=1}^{n} a_i)^k \leq \sum_{i=1}^{n} a_i^k \tag{13}$$

Lemma 7 *[28]:* For $a, b \in \mathbb{R}$, $\forall \epsilon > 0$, we have

$$ab \leq \frac{\epsilon^p}{p} \mid a \mid^p + \frac{1}{q\epsilon^q} \mid b \mid^q \tag{14}$$

where $p > 1$, $q > 1$ and $(p-1)(q-1) = 1$.

III. CONTROL DESIGN AND STABILITY ANALYSIS

A. CONTROL DESIGN OF ATTITUDE SYSTEM

For attitude control system, define the error variable as $Z_1 = X_1 - \Theta_d = [z_{\phi 1}, z_{\theta 1}, z_{\psi 1}]^T$, $Z_2 = Y_1 - \alpha_1 = [z_{\phi 2}, z_{\theta 2}, z_{\psi 2}]^T$ and $\tilde{Z}_1 = diag(z_{\phi 1}, z_{\theta 1}, z_{\psi 1})$, $\tilde{Z}_2 = diag(z_{\phi 2}, z_{\theta 2}, z_{\psi 2})$, where Θ_d is the desired value of Θ and $\alpha_1 \in R^{3\times 1}$ is virtual controller. Then, the time derivative of Z_1 is given by

$$\dot{Z}_1 = F_1(X_1, Y_1) + \Lambda_1 Y_1 - \dot{\Theta}_d \tag{15}$$

Step 1. Take the Lyapunov function candidate V_1 as

$$V_1 = \frac{1}{2} Z_1^T \Lambda_1^{-1} Z_1 \tag{16}$$

Differentiating V_1 yields

$$\dot{V}_1 = Z_1^T \Lambda_1^{-1} F_1(X_1, Y_1) + Z_1^T Z_2 + Z_1^T \alpha_1 - Z_1^T \Lambda_1^{-1} \dot{\Theta}_d \tag{17}$$

A virtual control signal is chosen as

$$\alpha_1 = -\tilde{Z}_1^{2\mu-1}\rho_1 + A_1 - \Lambda_1^{-1} F_1(X_1, Y_1) + \Lambda_1^{-1}\dot{\Theta}_d \tag{18}$$

where

$$A_1 = \begin{cases} \tilde{Z}_1 \bar{\beta}_1 + \tilde{Z}_1^3 \bar{\beta}_2 & \parallel Z_1 \parallel < \varepsilon_1 \\ -\tilde{Z}_1^{(2\nu-1)}\rho_2 & \parallel Z_1 \parallel \geq \varepsilon_1 \end{cases} \tag{19}$$

and $\mu = \frac{s_1}{s_2}$, $\nu = \frac{s_2}{s_1}$ and $s_1 > s_2 > 0$ are two odd numbers, $\bar{\beta}_1 = -(2-\nu)\varepsilon_1^{2\nu-2}\rho_2$ and $\bar{\beta}_2 = -(\nu-1)\varepsilon_1^{2\nu-4}\rho_2$. $\rho_1 = [\rho_{\phi 11}, \rho_{\theta 11}, \rho_{\psi 11}]^T$ and $\rho_2 = [\rho_{\phi 12}, \rho_{\theta 12}, \rho_{\psi 12}]^T$ are positive design parameter vectors with their element being positive constants, and ε_1 is the given error accuracy.

When $\parallel Z_1 \parallel \geq \varepsilon_1$, putting (18) into (17) shows

$$\dot{V}_1 = -Z_1^T \tilde{Z}_1^{2\mu-1}\rho_1 - Z_1^T \tilde{Z}_1^{2\nu-1}\rho_2 + Z_1^T Z_2 \tag{20}$$

When $\parallel Z_1 \parallel < \varepsilon_1$, we can get

$$\begin{aligned}
\dot{V}_1 &= -Z_1^T \tilde{Z}_1^{2\mu-1}\rho_1 - Z_1^T \tilde{Z}_1 \varepsilon_1^{2\nu-2}\rho_2(2-\nu) + Z_1^T Z_2 \\
&\quad -Z_1^T \tilde{Z}_1^3 \varepsilon_1^{2\nu-4}\rho_2(\nu-1) \\
&\leq -Z_1^T \tilde{Z}_1^{2\mu-1}\rho_1 - Z_1^T \tilde{Z}_1 \varepsilon_1^{2\nu-2}\rho_2(2-\nu) + Z_1^T Z_2 \\
&\quad -Z_1^T \tilde{Z}_1 \parallel \tilde{Z}_1 \parallel^2 \varepsilon_1^{2\nu-4}\rho_2(\nu-1) \\
&= -Z_1^T \tilde{Z}_1^{2\mu-1}\rho_1 - Z_1^T \tilde{Z}_1^{2\nu-1}\rho_2 + Z_1^T \tilde{Z}_1^{2\nu-1}\rho_2 + Z_1^T Z_2 \\
&\quad -Z_1^T \tilde{Z}_1 \varepsilon_1^{2\nu-2}\rho_2(2-\nu) \\
&\quad -Z_1^T \tilde{Z}_1 \parallel Z_1 \parallel^2 \varepsilon_1^{2\nu-4}\rho_2(\nu-1) \\
&\leq -Z_1^T \tilde{Z}_1^{2\mu-1}\rho_1 - Z_1^T \tilde{Z}_1^{2\nu-1}\rho_2 + Z_1^T \tilde{Z}_1^{2\nu-1}\rho_2 + Z_1^T Z_2 \\
&\quad -Z_1^T \tilde{Z}_1 \varepsilon_1^{2\nu-2}\rho_2(2-\nu) - Z_1^T \tilde{Z}_1 \varepsilon_1^{2\nu-2}\rho_2(\nu-1)
\end{aligned}$$

$$\leq -Z_1^T\tilde{Z}_1^{2\mu-1}\rho_1 - Z_1^T\tilde{Z}_1^{2\nu-1}\rho_2 + e_1\varepsilon_1^{2\nu}\rho_2 + Z_1^T Z_2 \tag{21}$$

with $e_1 = [1, 1, 1]$. In summary, one has

$$\dot{V}_1 \leq -Z_1^T\tilde{Z}_1^{2\mu-1}\rho_1 - Z_1^T\tilde{Z}_1^{2\nu-1}\rho_2 + Z_1^T Z_2 + e_1\varepsilon_1^{2\nu}\rho_2 \tag{22}$$

Remark 2: In the existing results, to get the finite-time stability of the closed-loop system, the design virtual control, i.e., α_1, includes the item $\tilde{Z}_1^{2\nu-1}$ with $0 < \nu < 1$. In backstepping design process, the next step will require the derivative of α_1. Note that $\frac{\tilde{Z}_1^{2\nu-1}}{dt} = (2\nu-1)\tilde{Z}_1^{2\nu-2}\dot{\tilde{Z}}_1$ and $2\nu - 2 < 0$. That means the derivative of α_1 may tend to infinity when $\tilde{Z}_1$ approaches to zero. This is called singularity problem of the derivative of virtual control. To avoid such a problem, here we construct α_1 as a piecewise function. By using interpolation method, the designed virtual control signal α_1 is continuous and differentiable at $||Z_1|| = \varepsilon_1$.

Step 2. Choose the Lyapunov function candidate V_2 as

$$V_2 = V_1 + \frac{1}{2}Z_2^T Z_2 + \frac{1}{2}\tilde{\theta}_2^T\beta_2\tilde{\theta}_2 \tag{23}$$

where $\tilde{\theta}_2 = \theta_2 - \hat{\theta}_2 = [\tilde{\theta}_{\phi 2}, \tilde{\theta}_{\theta 2}, \tilde{\theta}_{\psi 2}]^T$, $\hat{\theta}_2 = [\hat{\theta}_{\phi 2}, \hat{\theta}_{\theta 2}, \hat{\theta}_{\psi 2}]^T > 0$ is the estimate of $\theta_2 = [\| W_{\phi 2}^* \|^2, \| W_{\theta 2}^* \|^2, \| W_{\psi 2}^* \|^2]^T = [\theta_{\phi 2}, \theta_{\theta 2}, \theta_{\psi 2}]^T$. Define $\theta_{w2} = diag(\| W_{\phi 2}^* \|, \| W_{\theta 2}^* \|, \| W_{\psi 2}^* \|)$ and $\beta_2 = diag(\beta_{\phi 2}^{-1}, \beta_{\theta 2}^{-1}, \beta_{\psi 2}^{-1})$ with its elements are positive design parameter.

After a simple calculation, the time derivative of V_2 is given by

$$\dot{V}_2 = \dot{V}_1 + Z_2^T\dot{Z}_2 - \dot{\hat{\theta}}_2^T\beta_2\tilde{\theta}_2 \tag{24}$$

Further,

$$\dot{V}_2 = \dot{V}_1 + Z_2^T S_1 F_2(X_2) + Z_2^T B\tau + Z_2^T\tilde{S}_1 U - Z_2^T\dot{\alpha}_1 - \dot{\hat{\theta}}_2^T\beta_2\tilde{\theta}_2 \tag{25}$$

Define $U(X) = S_1 F_2(X_2) + B\tau - \dot{\alpha}_1$. By Lemma 2 we use neural networks to approximate $U(X)$ such that

$$U(X) = S_2(X)W_2^* + \delta_2(X) \tag{26}$$

where $W_2^* = [W_{\phi 2}^*, W_{\theta 2}^*, W_{\psi 2}^*]^T$ is the weight vector, $\delta_2(X) = [\delta_{\phi 2}(X_{\phi 2}), \delta_{\theta 2}(X_{\theta 2}), \delta_{\psi 2}(X_{\psi 2})]^T$ is the approximate error vector, $S_2(X) = diag(S_{\phi 2}(X_{\phi 2}), S_{\theta 2}(X_{\theta 2}), S_{\psi 2}(X_{\psi 2}))$ is the Gaussian radial basis function vector and $\| \delta_2(X) \| \leq \bar{\delta}_2$ with $\bar{\delta}_2 > 0$ being the accuracy level. Thus,

$$\dot{V}_2 = \dot{V}_1 + Z_2^T S_2(X)W_2^* + Z_2^T\delta_2(X) + Z_2^T\tilde{S}_1 U - \dot{\hat{\theta}}_2^T\beta_2\tilde{\theta}_2 \tag{27}$$

Using Young inequality, the following inequalities can be obtained.

$$\begin{aligned} Z_2^T S_2(X)W_2^* &= Z_2^T S_2(X)\theta_{w2}\theta_{w2}^{-1}W_2^* \\ &\leq \frac{1}{2a}Z_2^T S_2(X)\theta_{w2}\theta_{w2}^T S_2^T(X)Z_2 + \frac{3}{2}a \\ &\leq \frac{1}{2a}Z_2^T S_2(X)S_2^T(X)\tilde{Z}_2\theta_2 + \frac{3}{2}a \end{aligned} \tag{28}$$

$$Z_2^T\delta_2(X) \leq \frac{1}{2a}Z_2^T Z_2 + \frac{1}{2}a\bar{\delta}_2^2 \tag{29}$$

where a is a positive positive parameter.

Substituting (28) and (29) into (27) yields

$$\dot{V}_2 \leq \dot{V}_1 + \frac{1}{2a}Z_2^T S_2(X)S_2^T(X)\tilde{Z}_2\theta_2 + \frac{1}{2a}Z_2^T Z_2 + Z_2^T\tilde{S}_1 U - \dot{\hat{\theta}}_2^T\beta_2\tilde{\theta}_2 + \frac{3}{2}a + \frac{1}{2}a\bar{\delta}_2^2 \tag{30}$$

Hence, the controller U is designed as

$$U = -\tilde{S}_1^{-1}\tilde{Z}_2^{2\mu-1}\bar{\rho}_1 - \tilde{S}_1^{-1}\tilde{Z}_2^{2\nu-1}\bar{\rho}_2 - \tilde{S}_1^{-1}Z_1 - \frac{1}{2a}\tilde{S}_1^{-1}S_2(X)S_2^T(X)\tilde{Z}_2\hat{\theta}_2 - \frac{1}{2a}\tilde{S}_1^{-1}Z_2 \tag{31}$$

where $\bar{\rho}_1 = [\rho_{\phi 21}, \rho_{\theta 21}, \rho_{\psi 21}]^T$ and $\bar{\rho}_2 = [\rho_{\phi 22}, \rho_{\theta 22}, \rho_{\psi 22}]^T$, their elements are positive design parameters.

Then, replacing (31) into (30) shows

$$\begin{aligned} \dot{V}_2 \leq\ & \dot{V}_1 - Z_2^T\tilde{Z}_2^{2\mu-1}\bar{\rho}_2 - Z_2^T\tilde{Z}_2^{2\nu-1}\bar{\rho}_2 - Z_2^T Z_1 \\ & + \frac{1}{2a}Z_2^T S_2(X)S_2^T(X)\tilde{Z}_2\tilde{\theta}_2 - \dot{\hat{\theta}}_2^T\beta_2\tilde{\theta}_2 + \frac{3}{2}a \\ & + \frac{1}{2}a\bar{\delta}_2^2 \end{aligned} \tag{32}$$

The adaptive law $\hat{\theta}_2$ is designed as

$$\dot{\hat{\theta}}_2 = -\beta_2^{-1}\hat{\theta}_{\mu 1} - \beta_2^{-1}\hat{\theta}_{\nu 1} + \frac{1}{2a}(Z_2^T S_2(X)S_2^T(X)\tilde{Z}_2\beta_2^{-1})^T \tag{33}$$

where $\hat{\theta}_{\mu 1} = [\hat{\theta}_{\phi 2}^{2\mu-1}, \hat{\theta}_{\theta 2}^{2\mu-1}, \hat{\theta}_{\psi 2}^{2\mu-1}]^T$ and $\hat{\theta}_{\nu 1} = [\hat{\theta}_{\phi 2}^{2\nu-1}, \hat{\theta}_{\theta 2}^{2\nu-1}, \hat{\theta}_{\psi 2}^{2\nu-1}]^T$. Bringing (33) into (32) yields

$$\begin{aligned} \dot{V}_2 \leq\ & \dot{V}_1 - Z_2^T\tilde{Z}_2^{2\mu-1}\bar{\rho}_2 - Z_2^T\tilde{Z}_2^{2\nu-1}\bar{\rho}_2 + \hat{\theta}_{\mu 1}^T\tilde{\theta}_2 \\ & + \hat{\theta}_{\nu 1}^T\tilde{\theta}_2 - Z_2^T Z_1 + \frac{3}{2}a + \frac{1}{2}a\bar{\delta}_2^2 \end{aligned} \tag{34}$$

For $\hat{\theta}_{\mu 1}^T\tilde{\theta}_2$, by using Lemma 3, one has

$$\hat{\theta}_{\mu 1}^T\tilde{\theta}_2 = \tilde{\theta}_2^T\hat{\theta}_{\mu 1} = \tilde{\theta}_2^T\Upsilon_1 \leq \tilde{\mu}\theta_{\mu 2} - \tilde{\mu}\tilde{\theta}_{\mu 2} \tag{35}$$

where $\tilde{\mu} = [\frac{2\mu-1}{2\mu}, \frac{2\mu-1}{2\mu}, \frac{2\mu-1}{2\mu}]$, $\theta_{\mu 2} = [\theta_{\phi 2}^{2\mu}, \theta_{\theta 2}^{2\mu}, \theta_{\psi 2}^{2\mu}]^T$, $\tilde{\theta}_{\mu 2} = [\tilde{\theta}_{\phi 2}^{2\mu}, \tilde{\theta}_{\theta 2}^{2\mu}, \tilde{\theta}_{\psi 2}^{2\mu}]^T$ and $\Upsilon_1 = [(\theta_{\phi 2} - \tilde{\theta}_{\phi 2})^{2\mu-1}, (\theta_{\theta 2} - \tilde{\theta}_{\theta 2})^{2\mu-1}, (\theta_{\psi 2} - \tilde{\theta}_{\psi 2})^{2\mu-1}]^T$. By Lemma 1, one gets

$$\hat{\theta}_{\nu 1}^T\tilde{\theta}_2 = \tilde{\theta}_2^T\hat{\theta}_{\nu 1} = \tilde{\theta}_2^T\Upsilon_2 \leq D_0\theta_{\nu 2} - C_0\tilde{\theta}_{\nu 2} \tag{36}$$

where $c_0 = \frac{2^{\nu-1}}{1+\nu}(1 - 2^{\nu(\nu-1)})$, $\Upsilon_2 = [(\theta_{\phi 2} - \tilde{\theta}_{\phi 2})^{2\nu-1}, (\theta_{\theta 2} - \tilde{\theta}_{\theta 2})^{2\nu-1}, (\theta_{\psi 2} - \tilde{\theta}_{\psi 2})^{2\nu-1}]^T$, $d_0 = \frac{1}{1+\nu}(1 - 2^{2\nu-1} + \frac{1}{1+\nu}\nu + \frac{1}{1+\nu}2^{\nu}(1 - \nu^2))$, $D_0 = [d_0, d_0, d_0]$, $C_0 = [c_0, c_0, c_0]$, $\theta_{\nu 2} = [\theta_{\phi 2}^{2\nu}, \theta_{\theta 2}^{2\nu}, \theta_{\psi 2}^{2\nu}]^T$ and $\tilde{\theta}_{\nu 2} = [\tilde{\theta}_{\phi 2}^{2\nu}, \tilde{\theta}_{\theta 2}^{2\nu}, \tilde{\theta}_{\psi 2}^{2\nu}]^T$.

Thus, the following inequality holds.

$$\dot{V}_2 \leq \dot{V}_1 - Z_2^T\tilde{Z}_2^{2\mu-1}\bar{\rho}_2 - Z_2^T\tilde{Z}_2^{2\nu-1}\bar{\rho}_2 - \tilde{\mu}\tilde{\theta}_{\mu 2} - C_0\tilde{\theta}_{\nu 2} - Z_2^T Z_1 + C \tag{37}$$

where $C = \tilde{\mu}\theta_{\mu 2} + D_0\theta_{\nu 2} + \frac{3}{2}a + \frac{1}{2}a\bar{\delta}_2^2$.

B. STABILITY ANALYSIS OF ATTITUDE SYSTEM

At present stage, we summarize the above discussion to give the following theorem.

Theorem 1: Consider attitude control system (4) under the Assumptions 1-3. Then controller (31) associated with the virtual control signal (18) and adaptive law (33) will ensure the following conclusions hold.

1). The tracking error converges to a small neighborhood of the origin point in fixed time;

2). All the closed-loop signals remain bounded.

Proof: To prove Theorem 1, consider the Lyapunov function as below.

$$V_2 = \frac{1}{2}Z_1^T Z_1 + \frac{1}{2}Z_2^T Z_2 + \frac{1}{2}\tilde{\theta}_2^T \beta_2 \tilde{\theta}_2 \tag{38}$$

Let $\rho_m = min\{\beta_{\phi 2}^{-\mu}, \beta_{\theta 2}^{-\mu}, \beta_{\psi 2}^{-\mu}\}$. Then,

$$\begin{aligned} -\tilde{\mu}\tilde{\theta}_{\mu 2} \leq -(\frac{2\mu-1}{2\mu})2^{\mu}\rho_m[(2^{\mu}\beta_{\phi 2}^{\mu})^{-1}\tilde{\theta}_{\phi 2}^{2\mu} \\ +(2^{\mu}\beta_{\theta 2}^{\mu})^{-1}\tilde{\theta}_{\theta 2}^{2\mu} + (2^{\mu}\beta_{\psi 2}^{\mu})^{-1}\tilde{\theta}_{\psi 2}^{2\mu}] \end{aligned} \tag{39}$$

By using Lemma 6, one has

$$-\tilde{\mu}\tilde{\theta}_{\mu 2} \leq -a_{\mu}(\frac{1}{2}\tilde{\theta}_2\beta_2\tilde{\theta}_2^T)^{\mu}$$

where $a_{\mu} = (\frac{2\mu-1}{2\mu})2^{\mu}\rho_m 3^{1-\mu}$.

Similarly,

$$-C_0\tilde{\theta}_{\nu 2} \leq -a_{\nu}(\frac{1}{2}\tilde{\theta}_2^T\beta_2\tilde{\theta}_2)^{\nu} \tag{40}$$

where $\tilde{\rho}_m = min\{\beta_{\phi 2}^{-\nu}, \beta_{\theta 2}^{-\nu}, \beta_{\psi 2}^{-\nu}\}$, $a_{\nu} = c_0 2^{\nu}\tilde{\rho}_m$. And let $\rho_h = min(2^{\mu}\rho_{\phi 11}, 2^{\mu}\rho_{\theta 11}, 2^{\mu}\rho_{\psi 11}, 2^{\mu}\rho_{\phi 12}, 2^{\mu}\rho_{\theta 12}, 2^{\mu}\rho_{\psi 12}, a_{\mu})$ and $\rho_l = min(2^{\nu}\rho_{\phi 11}, 2^{\nu}\rho_{\theta 11}, 2^{\nu}\rho_{\psi 11}, 2^{\nu}\rho_{\phi 12}, 2^{\nu}\rho_{\theta 12}, 2^{\nu}\rho_{\psi 12}, a_{\nu})$.

Then, it follows immediately from using Lemma 5 and Lemma 6 to (37) that

$$\begin{aligned} \dot{V}_2 &\leq -\rho_h[3^{1-\mu}(\frac{1}{2}Z_1^T Z_1)^{\mu} + 3^{1-\mu}(\frac{1}{2}Z_2^T Z_2)^{\mu} \\ &\quad +(\frac{1}{2}\tilde{\theta}_2\beta_2\tilde{\theta}_2^T)^{\mu}] - \rho_l[(\frac{1}{2}Z_1^T Z_1)^{\nu} + (\frac{1}{2}Z_2^T Z_2)^{\nu} \\ &\quad +(\frac{1}{2}\tilde{\theta}_2\beta_2\tilde{\theta}_2^T)^{\nu}] + C \\ &\leq -\tilde{\rho}_h(\frac{1}{2}Z_1^T Z_1 + \frac{1}{2}Z_2^T Z_2 + \frac{1}{2}\tilde{\theta}_2\beta_2\tilde{\theta}_2^T)^{\mu} \\ &\quad -\rho_l(\frac{1}{2}Z_1^T Z_1 + \frac{1}{2}Z_2^T Z_2 + \frac{1}{2}\tilde{\theta}_2\beta_2\tilde{\theta}_2^T)^{\nu} + C \\ &= -\tilde{\rho}_h V_2^{\mu} - \rho_l V_2^{\nu} + C \end{aligned} \tag{41}$$

where $\tilde{\rho}_h = min\{3^{1-\mu}\rho_h, \rho_h\}$.

Thus, the fixed-time stability of the attitude system is derived from Lemma 4.

C. CONTROL DESIGN OF POSITION SYSTEM

For position control system, define error $\xi_1 = X_2 - X_d = [\xi_{x1}, \xi_{y1}, \xi_{z1}]^T$, $\xi_2 = Y_2 - \alpha_2 = [\xi_{x2}, \xi_{y2}, \xi_{z2}]^T$, $\tilde{\xi}_1 = diag(\xi_{x1}, \xi_{y1}, \xi_{z1})$, $\tilde{\xi}_2 = diag(\xi_{x2}, \xi_{y2}, \xi_{z2})$.

By following the same line used in the design procedure of the attitude control system, the virtual controller $\alpha_2 \in R^{3\times 1}$, controller $\tilde{U}$ and adaptive law $\hat{\vartheta}_2 \in R^{3\times 1}$ of the position system can be constructed as follows.

$$\alpha_2 = -\tilde{\xi}_1^{2\mu-1}\lambda_1 + \tilde{A}_1 + \dot{X}_d \tag{42}$$

where

$$\tilde{A}_1 = \begin{cases} \tilde{\xi}_1\tilde{\beta}_1 + \tilde{\xi}_1^3\tilde{\beta}_2 & \| \xi_1 \| < \varepsilon_2 \\ -\tilde{\xi}_1^{(2\nu-1)}\lambda_2 & \| \xi_1 \| \geq \varepsilon_2 \end{cases} \tag{43}$$

and $\mu = \frac{s_1}{s_2}$, $\nu = \frac{s_2}{s_1}$, $s_1 > s_2 > 0$ are two odd numbers, $\tilde{\beta}_1 = -(2-\nu)\varepsilon_2^{2\nu-2}\lambda_2$, $\tilde{\beta}_2 = -(\nu-1)\varepsilon_2^{2\nu-4}\lambda_2$, $\lambda_1 = [\rho_{x11}, \rho_{y11}, \rho_{z11}]^T$, $\lambda_2 = [\rho_{x12}, \rho_{y12}, \rho_{z12}]^T$ with their elements being positive design parameters and ε_2 being the given error accuracy.

$$\begin{aligned} \tilde{U} = -\tilde{\xi}_2^{2\mu-1}\tilde{\lambda}_1 - \tilde{\xi}_2^{2\nu-1}\tilde{\lambda}_2 - \frac{1}{2\tilde{a}}\xi_2 - \xi_1 \\ -\frac{1}{2\tilde{a}}\xi_2^T\tilde{S}_2(X)\tilde{S}_2^T(X)\tilde{\xi}_2\hat{\vartheta}_2 \end{aligned} \tag{44}$$

where $\tilde{\lambda}_1 = [\rho_{x21}, \rho_{y21}, \rho_{z21}]^T$, $\tilde{\lambda}_2 = [\rho_{x22}, \rho_{y22}, \rho_{z22}]^T$, its elements are positive constants, $\tilde{a}$ is a positive parameter and $\tilde{S}_2(X) = diag(S_{x2}(X_{x2}), S_{y2}(X_{y2}), S_{z2}(X_{z2}))$ is the Gaussian radial basis function matrix.

Define $\tilde{\vartheta}_2 = \vartheta_2 - \hat{\vartheta}_2 = [\tilde{\vartheta}_{x2}, \tilde{\vartheta}_{y2}, \tilde{\vartheta}_{z2}]^T$, where $\hat{\vartheta}_2 = [\hat{\vartheta}_{\phi 2}, \hat{\vartheta}_{\theta 2}, \hat{\vartheta}_{\psi 2}]^T > 0$ is the estimate of $\vartheta_2 = [\| W_{x2}^* \|^2, \| W_{y2}^* \|^2, \| W_{z2}^* \|^2]^T = [\vartheta_{x2}, \vartheta_{y2}, \vartheta_{z2}]^T$, and $\chi_2 = diag(\beta_{x2}^{-1}, \beta_{y2}^{-1}, \beta_{z2}^{-1})$ is a matrix, which elements are positive design parameters.

$$\dot{\hat{\vartheta}}_2 = -\chi_2^{-1}\hat{\vartheta}_{\mu 1} - \chi_2^{-1}\hat{\vartheta}_{\nu 1} + \frac{1}{2\tilde{a}}(\xi_2^T\tilde{S}_2(X)\tilde{S}_2^T(X)\tilde{\xi}_2\chi_2^{-1})^T \tag{45}$$

where $\hat{\vartheta}_{\mu 1} = [\hat{\vartheta}_{x1}^{2\mu-1}, \hat{\vartheta}_{y1}^{2\mu-1}, \hat{\vartheta}_{z1}^{2\mu-1}]^T$ and $\hat{\vartheta}_{\nu 1} = [\hat{\vartheta}_{x1}^{2\nu-1}, \hat{\vartheta}_{y1}^{2\nu-1}, \hat{\vartheta}_{z1}^{2\nu-1}]^T$.

D. STABILITY ANALYSIS OF POSITION SYSTEM

Theorem 2: Consider position control system (5) under the Assumptions 1-3. Then controller (44) associated with the virtual control signal (42) and adaptive law (45) will ensure the following conclusions hold.

1). The tracking error converges to a small neighborhood of the origin point in fixed time;

2). All the closed-loop signals remain bounded.

Proof: The process of control design and stability analysis of the position control system is as the same as the one of the attitude system. So, it is omitted here.

IV. SIMULATION

In this section, we will perform simulation study to verify the effectiveness of the proposed control scheme. The parameters of quadrotor are give by Table 1.

The desired trajectory (the corresponding length unit is meter) is shown by the mathematical equations: $[x_d = 0, y_d = 0, z_d = t, (0 - 20s)]$; $[x_d = (t-20)cos\bar{\theta},$

$y_d = (t-20)sin\bar{\theta}$, $z_d = 20$, $(20-30s)$]; [$x_d = 10 + rcost$, $y_d = 11 + rsint$, $z_d = 20 - (t-30)$, $(30-45s)$]; [$x_d = 10 + rcos(45)$, $y_d = 11 + rsin(45)$, $z_d = -t$, $(45-50s)$], where $\bar{\theta} = \frac{\pi}{4}$, $r = 1$. The desired yaw angle is $\psi_d = 0$. That means the quadrotor will first rise vertically for 20 seconds to reach a height, then maintain this height and flies at a certain angle between x and y axes for 10 seconds, and then makes a descent spiral, finally, drop vertically to the ground. In simulation, the initial values are: $x(0) = (0, \ldots, 0)^T$ and $\hat{\theta}_2(0) = 0$. The controller parameters are $\mu = 1.01$, $\nu = 0.99$ $n = 60$, $\psi_d = 0$, $\hat{\vartheta}_2(0) = 0$ and ω_i $(i = 1, .., \lambda)$ is $\sqrt{2}$ and $a = \tilde{a} = 1$. The centers of neural network are chosen as $-2; -1; 0; 1; 2$, to construct the basis vector functions of RBF NNs. Simulation results are shown by Fig.s $(2) - (5)$, the quadcopter perfectly tracks the desired trajectory of the x, y and z axes, and from Fig.s $(6) - (8)$ we can see that he various attitude angles of the quadcopter are also well tracked to the desired attitude angles, and the sudden change caused by the trajectory change point can also be tracked faster.

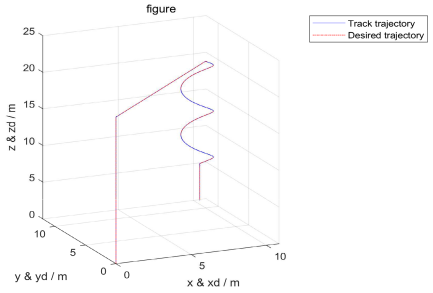

FIGURE 2. Tracking situation.

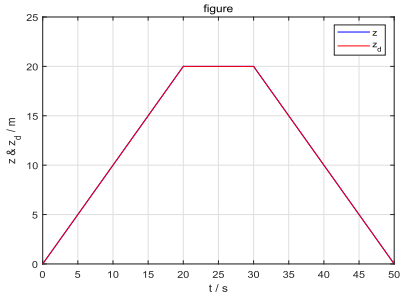

FIGURE 3. Tracking curve along Z axis.

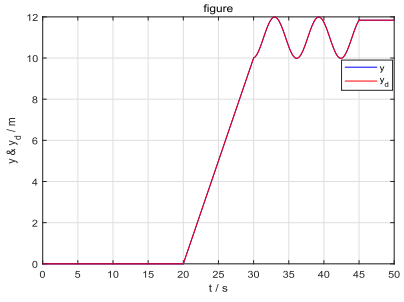

FIGURE 4. Tracking curve along Y axis.

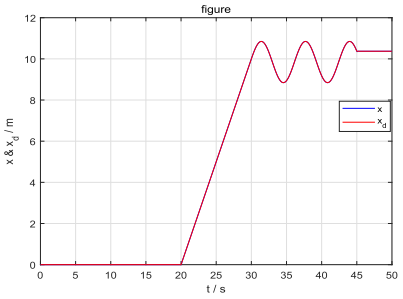

FIGURE 5. Tracking curve along X axis.

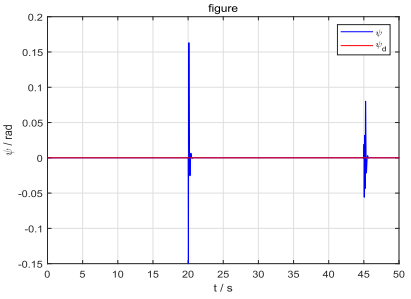

FIGURE 6. Yaw angle curve.

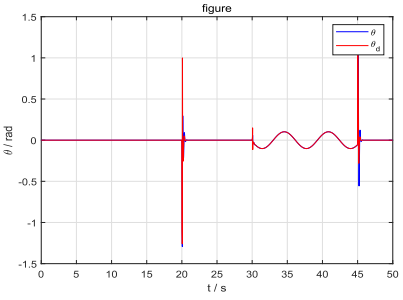

FIGURE 7. Pitch angle curve.

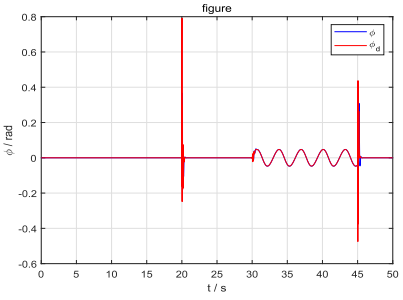

FIGURE 8. Roll angle curve.

Remark 3: In the control design, the gyro torque produced by gyroscopic effect is considered as the uncertain factors, which is usually determined by the motor speed ϖ. In simulation its form is taken as $\tau_{uc} = \Sigma_{i=1}^{4} \varpi_i J_{rz} \Omega \times e_3$, where J_{rz} is an element of the inertial diagonal array $J_r = diag(J_{rx}, J_{ry}, J_{rz})$ of each rotor. Therefore, in order to calculate the specific form of gyro torque in simulation, as done

in [29] the rotor speed is given by.

$$\begin{bmatrix} \varpi_1^2 \\ \varpi_2^2 \\ \varpi_3^2 \\ \varpi_4^2 \end{bmatrix} = \begin{bmatrix} \frac{1}{4}C_T & 0 & -\frac{1}{2}lC_T & \frac{1}{4}C_Q \\ \frac{1}{4}C_T & \frac{1}{2}lC_T & 0 & -\frac{1}{4}C_Q \\ \frac{1}{4}C_T & 0 & \frac{1}{2}lC_T & \frac{1}{4}C_Q \\ \frac{1}{4}C_T & -\frac{1}{2}lC_T & 0 & -\frac{1}{4}C_Q \end{bmatrix} \times \begin{bmatrix} U_1 \\ U_2 \\ U_3 \\ U_4 \end{bmatrix} \quad (46)$$

where ϖ_i $(i = 1, 2, 3, 4)$ are desired rotor speed, C_T is the lift coefficient of the rotor, C_Q is the anti-torque coefficient, l is the distance from the motor to the center of mass. And the form of f_{uc} is $f_{uc} = -C_{da} \mid V \mid V$, where $C_{da} = 0.5\rho_{air}C_d$, ρ_{air} is air density and C_d is the drag coefficient. Besides, in order to avoid the trouble of deriving the desired roll angle, pitch angle and Yaw angle, we introduce a filter to track their derivatives.

$$\Lambda = \begin{cases} \dot{\zeta}_1 = \varsigma_2 \\ \dot{\varsigma}_2 = -2s\varsigma_2 - 2s^2(\zeta_1 - u(t)) \end{cases}$$

where ζ_1 and ς_2 are state variables, s is a positive constant and $u(t)$ is the input signal.

TABLE 1. Parameters.

Parameter	Value	Unit
J_x	$4.6235 * 10^{-3}$	kgm^2
J_y	$4.6235 * 10^{-3}$	kgm^2
J_z	$6.2546 * 10^{-3}$	kgm^2
J_{rz}	$6.0354 * 10^{-5}$	kgm^2
C_T	$4.0298 * 10^{-5}$	
C_Q	$3.531 * 10^{-7}$	
l	0.2	m
g	9.806	m/s^2
m	0.5	kg
ρ_{air}	1.29	kg/m^3
C_{da}	$5.623 * 10^{-4}$	
$\rho_{\phi 11}$	21	
$\rho_{\theta 11}$	21	
$\rho_{\psi 11}$	21	
ρ_{x11}	21	
ρ_{y11}	21	
ρ_{z11}	21	
$\rho_{\phi 12}$	3	
$\rho_{\theta 12}$	3	
$\rho_{\psi 12}$	3	
ρ_{x12}	3	
ρ_{y12}	3	
ρ_{z12}	3	
$\rho_{\phi 21}$	21	
$\rho_{\theta 21}$	21	
$\rho_{\psi 21}$	21	
ρ_{x21}	21	
ρ_{y21}	21	
ρ_{z21}	21	
$\rho_{\phi 22}$	3	
$\rho_{\theta 22}$	3	
$\rho_{\psi 22}$	3	
ρ_{x22}	3	
ρ_{y22}	3	
ρ_{z22}	3	
β_{x2}	7	
β_{y2}	7	
β_{z2}	7	
$\beta_{\phi 2}$	7	
$\beta_{\theta 2}$	7	
$\beta_{\psi 2}$	7	

V. CONCLUSION

In this research, we address the problem of trajectory tracking control of a quadrotor. Based on adaptive neural control approach a fixed-time backstepping control design proces is proposed for the quadrotor. The proposed adaptive neural controller ensures that the quadrotor achieves the trajectory tracking issue in finite time. Particularly, the design virtual control signals avoid the derivative singularity problem. At last, a numerical simulation is used to verify the effectiveness of the proposed control scheme.

APPENDIX. PARAMETERS

See Table 1.

REFERENCES

[1] F. Yacef, O. Bouhali, and M. Hamerlain, "Adaptive fuzzy backstepping control for trajectory tracking of unmanned aerial quadrotor," in *Proc. Int. Conf. Unmanned Aircr. Syst. (ICUAS)*, May 2014, pp. 920–927.
[2] Y. Zhang, Z. Chen, X. Zhang, Q. Sun, and M. Sun, "A novel control scheme for quadrotor UAV based upon active disturbance rejection control," *Aerosp. Sci. Technol.*, vol. 79, pp. 601–609, Aug. 2018.
[3] H. Razmi and S. Afshinfar, "Neural network-based adaptive sliding mode control design for position and attitude control of a quadrotor UAV," *Aerosp. Sci. Technol.*, vol. 91, pp. 12–27, Aug. 2019.
[4] N. Wang and Q. Deng, "Non-singular terminal sliding mode tracking control of a quadrotor with external disturbances," in *Proc. IEEE 8th Annu. Int. Conf. CYBER Technol. Autom., Control, Intell. Syst. (CYBER)*, Jul. 2018, pp. 1254–1259.
[5] X. Wentao, T. Shaojun, and Y. Hui, "Robust trajectory tracking control for a quadrotor based on a composite sliding mode control method," in *Proc. 37th Chin. Control Conf. (CCC)*, Jul. 2018, pp. 919–924.
[6] E. Kayacan and R. Maslim, "Type-2 fuzzy logic trajectory tracking control of quadrotor VTOL aircraft with elliptic membership functions," *IEEE/ASME Trans. Mechatronics*, vol. 22, no. 1, pp. 339–348, Feb. 2017.
[7] H. Nguyen Dang, B. Mohamed, and H. Rafaralahy, "Trajectory-tracking control design for an under-actuated quadrotor," in *Proc. Eur. Control Conf. (ECC)*, Jun. 2014, pp. 1765–1770.
[8] J. Xu, P. Shi, C.-C. Lim, C. Cai, and Y. Zou, "Reliable tracking control for under-actuated quadrotors with wind disturbances," *IEEE Trans. Syst., Man, Cybern. Syst.*, vol. 49, no. 10, pp. 2059–2070, Oct. 2019.
[9] Y. Zou and B. Zhu, "Adaptive trajectory tracking controller for quadrotor systems subject to parametric uncertainties," *J. Franklin Inst.*, vol. 354, no. 15, pp. 6724–6746, Oct. 2017.
[10] X. Shao, J. Liu, and H. Wang, "Robust back-stepping output feedback trajectory tracking for quadrotors via extended state observer and sigmoid tracking differentiator," *Mech. Syst. Signal Process.*, vol. 104, pp. 631–647, May 2018.
[11] X. Shao, Q. Meng, J. Liu, and H. Wang, "RISE and disturbance compensation based trajectory tracking control for a quadrotor UAV without velocity measurements," *Aerosp. Sci. Technol.*, vol. 74, pp. 145–159, Mar. 2018.
[12] D. J. Almakhles, "Robust backstepping sliding mode control for a quadrotor trajectory tracking application," *IEEE Access*, vol. 8, pp. 5515–5525, 2020.
[13] O. García, P. Ordaz, O.-J. Santos-Sánchez, S. Salazar, and R. Lozano, "Backstepping and robust control for a quadrotor in outdoors environments: An experimental approach," *IEEE Access*, vol. 7, pp. 40636–40648, 2019.

[14] D. Wu, H. Du, and W. Zhu, "Finite-time position tracking control of a quadrotor aircraft," in *Proc. 36th Chin. Control Conf. (CCC)*, Jul. 2017, pp. 737–742.
[15] X.-N. Shi, Y.-A. Zhang, and D. Zhou, "Almost-global finite-time trajectory tracking control for quadrotors in the exponential coordinates," *IEEE Trans. Aerosp. Electron. Syst.*, vol. 53, no. 1, pp. 91–100, Feb. 2017.
[16] X. Zheng, Z. Wang, and T. Zhang, "Robust finite-time attitude tracking control for nonlinear quadrotor with uncertainties and delays," in *Proc. IEEE Int. Conf. Robot. Biomimetics (ROBIO)*, Dec. 2017, pp. 1775–1780.
[17] W.-T. Xue, S.-J. Tao, and X.-F. Yang, "Trajectory tracking controller design for a quadrotor aircraft based on cascade sliding mode control," in *Proc. IEEE 27th Int. Symp. Ind. Electron. (ISIE)*, Jun. 2018, pp. 994–999.
[18] Z. Zhou, H. Wang, Z. Hu, Y. Wang, and H. Wang, "A multi-time-scale finite time controller for the quadrotor UAVs with uncertainties," *J. Intell. Robot. Syst.*, vol. 94, no. 2, pp. 521–533, May 2019.
[19] B. Tian, Y. Ma, L. Liu, and Q. Zong, "Adaptive multivariable finite-time attitude control for quadrotor UAV," in *Proc. 37th Chin. Control Conf. (CCC)*, Jul. 2018, pp. 9792–9796.
[20] Y. Bai and C. Zhang, "Finite-time tracking control of a quadrotor UAV without velocity measurement," in *Proc. 2nd Int. Conf. Robot. Autom. Eng. (ICRAE)*, Dec. 2017, pp. 234–238.
[21] Q. Xu, Z. Wang, and Z. Zhen, "Adaptive neural network finite time control for quadrotor UAV with unknown input saturation," *Nonlinear Dyn.*, vol. 98, no. 3, pp. 1973–1998, Nov. 2019.
[22] X. Ai and J. Yu, "Fixed-time trajectory tracking for a quadrotor with external disturbances: A flatness-based sliding mode control approach," *Aerosp. Sci. Technol.*, vol. 89, pp. 58–76, Jun. 2019.
[23] B. Chen and C. Lin, "Finite-time stabilization-based adaptive fuzzy control design," *IEEE Trans. Fuzzy Syst.*, early access, Apr. 29, 2020, doi: 10.1109/TFUZZ.2020.2991153.
[24] B. Chen, H. Zhang, and C. Lin, "Observer-based adaptive neural network control for nonlinear systems in nonstrict-feedback form," *IEEE Trans. Neural Netw. Learn. Syst.*, vol. 27, no. 1, pp. 89–98, Jan. 2016.
[25] F. Wang and G. Lai, "Fixed-time control design for nonlinear uncertain systems via adaptive method," *Syst. Control Lett.*, vol. 140, Jun. 2020, Art. no. 104704.
[26] G. Hardy, J. Littlewood, and G. Pólya, *Inequalities*. Cambridge, U.K.: Cambridge Univ. Press, 1988.
[27] Z. Zuo and L. Tie, "A new class of finite-time nonlinear consensus protocols for multi-agent systems," *Int. J. Control*, vol. 87, no. 2, pp. 363–370, Feb. 2014.
[28] X. Jin, "Adaptive fixed-time control for MIMO nonlinear systems with asymmetric output constraints using universal barrier functions," *IEEE Trans. Autom. Control*, vol. 64, no. 7, pp. 3046–3053, Jul. 2019.
[29] W. Lei, C. Li, and M. Z. Q. Chen, "Robust adaptive tracking control for quadrotors by combining PI and self-tuning regulator," *IEEE Trans. Control Syst. Technol.*, vol. 27, no. 6, pp. 2663–2671, Nov. 2019.

MINGYU WANG received the Bachelor of Engineering degree in automation from Suihua University, in 2019. He is currently pursuing the degree with the School of Automation, Qingdao University, Qingdao, China. His research interests include nonlinear control systems, robust control, and adaptive fuzzy control.

BING CHEN received the B.A. degree in mathematics from Liaoning University, China, in 1982, the M.A. degree in mathematics from the Harbin Institute of Technology, China, in 1991, and the Ph.D. degree in electrical engineering from Northeastern University, China, in 1998. He is currently a Professor with the Institute of Complexity Science, Qingdao University, Qingdao, China. His research interests include nonlinear control systems, robust control, and adaptive fuzzy control.

CHONG LIN (Senior Member, IEEE) received the B.Sci. and M.Sci. degrees in applied mathematics from Northeastern University, China, in 1989 and 1992, respectively, and the Ph.D. degree in electrical and electronic engineering from Nanyang Technological University, Singapore, in 1999. He was a Research Associate with the Department of Mechanical Engineering, The University of Hong Kong, in 1999. From 2000 to 2006, he was a Research Fellow with the Department of Electrical and Computer Engineering, National University of Singapore. Since 2006, he has been a Professor with the Institute of Complexity Science, Qingdao University, China. He has published more than 60 research articles. He has coauthored two monographs. His current research interests include systems analysis and control, robust control, and fuzzy control.